ACADEMIC PRESS

Available online at www.sciencedirect.com
SCIENCE DIRECT®

DEVELOPMENTAL BIOLOGY

Developmental Biology 258 (2003) 291–306

www.elsevier.com/locate/ydbio

Positional cloning of a temperature-sensitive mutant *emmental* reveals a role for Sly1 during cell proliferation in zebrafish fin regeneration

Alex Nechiporuk,[a,1,*] Kenneth D. Poss,[a,1] Stephen L. Johnson,[b] and Mark T. Keating[a,*]

[a] *Howard Hughes Medical Institute, Department of Cardiology, Children's Hospital, Department of Cell Biology, Harvard Medical School, Boston, MA 02115, USA*
[b] *Department of Genetics, Washington University School of Medicine, St. Louis, MO 63110, USA*

Received for publication 25 October 2002, revised 20 February 2003, accepted 24 February 2003

Abstract

Here, we used classical genetics in zebrafish to identify temperature-sensitive mutants in caudal fin regeneration. Gross morphological, histological, and molecular analyses revealed that one of these strains, *emmental (emm)*, failed to form a functional regeneration blastema. Inhibition of emm function by heat treatment during regenerative outgrowth rapidly blocked regeneration. This block was associated with reduced proliferation in the proximal blastema and expansion of the nonproliferative distal blastemal zone. Positional cloning revealed that the *emm* phenotype is caused by a mutation in the orthologue of yeast *sly1*, a gene product involved in protein trafficking. *sly1* is upregulated in the newly formed blastema as well as during regenerative outgrowth. Thus, *sly1* is essential for blastemal organization and proliferation during two stages of fin regeneration.

Keywords: Zebrafish; Genetics; Regeneration; Fin; Blastema; Sly1; *emmental*

Introduction

Urodele amphibians and teleost fish are among certain lower vertebrate species that can regenerate multiple organs, including limb (fin), optic nerve, lens, and spinal cord. In contrast, mammalian regenerative abilities are limited. Despite the importance of this phenomenon, molecular and cellular mechanisms of regeneration are poorly understood. The zebrafish caudal fin is an excellent model for studying regeneration. It is a relatively simple, symmetrical organ composed of multiple fin rays (Becerra et al., 1983, 1996; Montes et al., 1982). Each ray consists of a pair of concave hemirays, surrounding mesenchymal tissue, including fibroblasts, scleroblasts (bone-secreting cells), pigment cells, blood vessels, and nerves. Fin regeneration in zebrafish is reliably completed within a wide temperature range (25–33°C) (Becerra et al., 1983; Geraudie and Singer, 1992; Johnson and Bennett, 1999; Poss et al., 2000b). At 33°C, it progresses through (1) wound healing and establishment of wound epithelium (0–12 h postamputation, hpa); (2) reorganization and proliferation of underlying mesenchymal tissues that results in formation of the blastema, a mass of pluripotent mesenchymal cells (12–48 hpa); (3) differentiation and outgrowth of the regenerate (beyond 48 hpa). It is thought that factor(s) released from the wound epidermis initiate and maintain blastemal proliferation (Poss et al., 2000a, b).

Large-scale mutagenesis screens in zebrafish have typically involved a classical, three-generation approach, with the aim of finding strong alleles that cause a lethal phenotype during development (Driever et al., 1996; Haffter et al., 1996; van Eeden et al., 1999). To analyze fin regeneration, it is advantageous to identify nonlethal mutations that may be temperature-sensitive in adult zebrafish. For instance, Johnson and Weston (1995) performed a parthenogenetic screen in zebrafish and isolated several temperature-sensi-

* Corresponding authors. Fax: +1-671-730-8317.
E-mail address: anechipo@enders.tch.harvard.edu (A. Nechiporuk). mkeating@enders.tch.harvard.edu (M.T. Keating).
[1] These authors contributed equally to this work.

0012-1606/03/$ – see front matter © 2003 Elsevier Science (USA). All rights reserved.
doi:10.1016/S0012-1606(03)00129-5

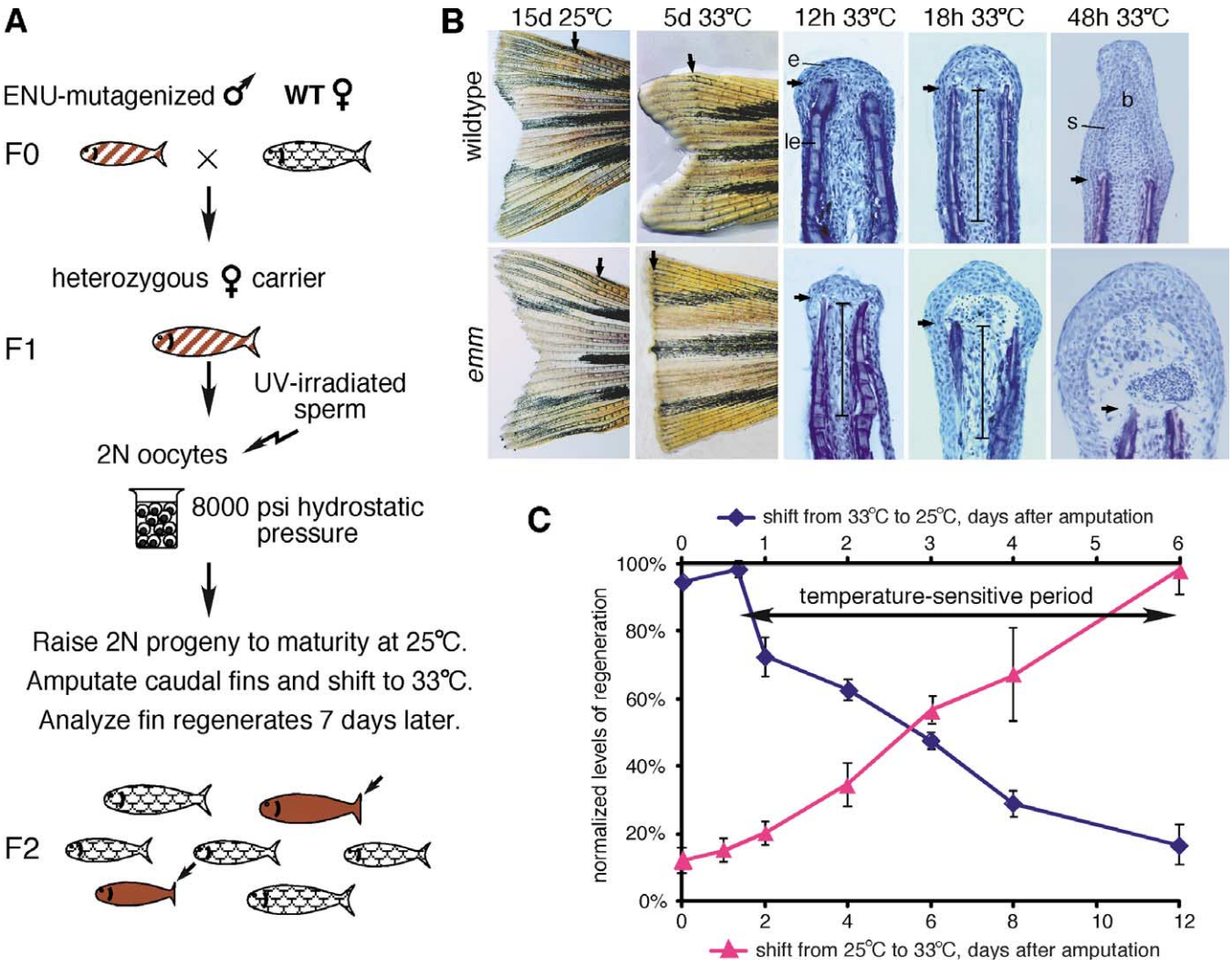

Fig. 1. Early pressure genetic screen to reveal regeneration mutants. (A) Illustration of "Early Pressure" (EP) temperature-sensitive (TS) mutagenesis screen. Male fish were mutagenized with ENU and crossed to wildtype females. ENU heterozygous progeny were subjected to EP gynogenesis. EP progeny were raised to maturity and examined for stage-specific fin regeneration defects at the nonpermissive temperature of 33°C. (B) Whole-mount (4 left panels, 15- and 5-day postamputation; anterior is at right) and histological (longitudinal sections of 12-, 18-, and 48-hpa fins stained with hematoxylin; anterior is at bottom) analyses of *emm* fin regenerates. Fish were preincubated at 33°C for 24 h before collecting regenerates at 12 and 18 hpa. Formation of the wound epidermis (arrowheads) and tissue disorganization (bracket) was not affected by *emm*, but *emm* blocked blastema formation. Note the dysmorphic, accellular blastema in *emm* regenerates (18 and 48 hpa). (C) Forward (red) and reverse (blue) temperature shift experiments. Five *emm* and five heterozygous sibling fish were shifted to the restrictive temperature at varying time points after caudal fin amputation. In reverse shift experiments, fish were held at the restrictive temperature for 1 day before the experiment. Caudal fins of *emm* and heterozygous siblings were then amputated, and five fish were shifted to the permissive temperature at various time points. In each case, the length of the regenerate was measured 2 days after the forward shift and 4 days after the reverse shift. The lengths of the regenerate for each time point from *emm* fish were averaged and then normalized to values obtained from controls. Data points are shown as mean ± SEM. Note that the *emm* temperature-sensitive period includes the blastema formation and regenerative outgrowth (beyond 18 hpa), but not wound-healing stages. The amputation plane is designated by black arrows. Abbreviations: b, blastema; e, epidermis; le, lepidotrichia; s, scleroblasts. Original magnification in (B): whole-mounts, 10×; sections, 180×.

tive (TS) mutations that disrupted fin regeneration and normal development.

In light of previous zebrafish embryonic screens (Golling et al., 2002; Haffter et al., 1996), one would expect that regeneration mutants can be subdivided into at least two general classes. One class would represent mutations in genes with specific roles in fin regeneration. For example, wound-healing genes would comprise molecules involved in regulation of epithelial cell migration, maturation of the wound epidermis, and establishment of epidermal–mesenchymal signaling. Genes that instruct blastema formation would control tissue dedifferentiation and proliferation. Finally, genes that are required for regenerative outgrowth maintain blastemal function or regulate cellular differentiation and patterning. A second class of mutants would represent mutations in genes required for basic cell functions, or general adult physiology and survival (e.g., vesicular trafficking, energy metabolism, cell cycle progression, and

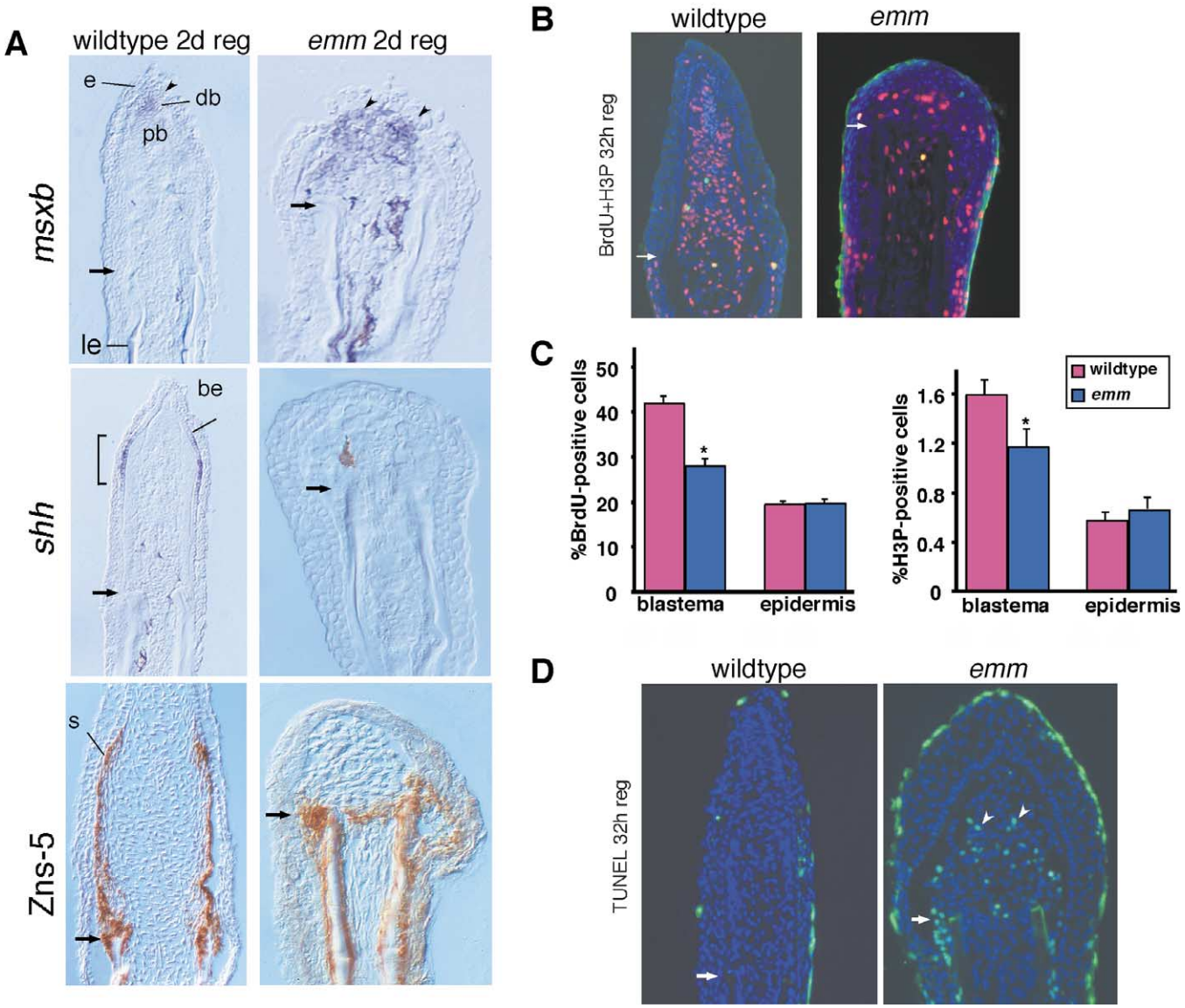

Fig. 2. *emm* fins fail to form mature blastema. The distal, regenerating end is at top. (A) Nomarski photographs of longitudinal sections from 2-day wildtype (left) and mutant (right) regenerates stained with *msxb* or *shh* antisense riboprobe (n = 6-12, violet) and Zns-5 antibody (n = 6-12, brown) are shown. Note that *msxb* expression is restricted to the distal blastema in wildtype regenerates, whereas *msxb* expression is diffuse in *emm*, indicating problems with blastema organization. Also, *emm* fins fail to express *shh*, and scleroblasts are not aligned, as indicated by diffuse, disorganized Zns-5 staining. (B) Longitudinal sections from wildtype and *emm* regenerates that have been processed for detection of BrdU (red) and H3P (green), and counterstained with DAPI (blue). Fins were treated with BrdU for 6 h before harvesting at 32 hpa. (C) Indices of proliferation in the blastema and epidermis of wildtype and *emm* regenerates during blastema formation. The percentage of BrdU- and H3P-positive cells was obtained by counting 8,000-12,000 DAPI-positive nuclei from 10 sections each of 4–5 immunostained regenerates. Note that the number of proliferating *emm* blastemal cells is reduced, but that epidermal proliferation is unaffected, suggesting a specific role for emm in blastemal proliferation. Results are shown as mean ± SEM (*$P < 0.001$, t test). (D) Longitudinal sections of wildtype (left) and *emm* (right) regenerates at 32 hpa, processed for TdT-mediated dUTP nick-end labeling (TUNEL; green). Sections were counterstained with DAPI (blue). Note a significant number of blastemal cells undergoing apoptosis in *emm* regenerates (arrowheads) (*emm:* 10.17 ± 2.09% versus wt: 1.5 ± 0.57%; $P < 0.014$, t test; the percentages of TUNEL-positive cells were obtained by analyzing 3–6 sections from 4 different regenerates). Abbreviations: be, basal epidermis; db, distal blastema; e, epidermis; pb, proximal blastema; s, scleroblasts. Original magnification in (A-C) is 180×.

hormonal signaling). Thus, genetic dissection of regeneration can facilitate our understanding of control mechanisms during vertebrate regeneration, as well as produce novel reagents that can be applied to understand basic cellular processes.

Here, we used an "Early Pressure" mutagenesis screen to produce TS mutants that have stage-specific defects in caudal fin regeneration. One of these mutants, *emmental*, displayed a regenerative block during blastema formation. We isolated *emm* by positional cloning and discovered that it encodes an orthologue of yeast *sly1*, a gene important for intracellular protein and vesicle transport (Dascher et al., 1991; Halachmi and Lev, 1996; Mizuta and Warner, 1994). We show that *emm* is required for blastemal proliferation

and organization during blastema formation and regenerative outgrowth.

Materials and methods

Mutagenesis screen

Males of the SJD or C32 inbred lines (Nechiporuk et al., 1999) were mutagenized with *N*-ethyl-*N*-nitrosourea (ENU) by using published protocols (Solnica-Krezel et al., 1994). Mutagenized males were mated to females of a different genetic background. We estimated germ-line mutation rates at $\sim 5 \times 10^{-3}$ by crossing mutagenized males to *sparse* females and examining their progeny for absence of pigmentation. ENU heterozygous females were subjected to early pressure parthenogenesis (Streisinger et al., 1981). We generated 2050 mature EP progeny from 227 F_1 ENU-heterozygous females. The resulting families were raised at 25°C until 2–3 months of age. Then, 50% of the caudal fin was amputated from each fish, and families were shifted to the restrictive temperature, 33°C. One week later, each fish was analyzed for regeneration defects under a dissecting microscope (Fig. 1A). We identified 11 potential founders that had defects in caudal fin regeneration. One *emm* founder was isolated from a family of 8. The founder fish showed a consistent regeneration block at the restrictive temperature and was outcrossed to wildtype fish for further genetic analysis.

Wildtype fin regeneration at 33°C has been previously characterized (Johnson and Weston, 1995; Nechiporuk and Keating, 2002; Poss et al., 2002). Regeneration is consistently completed without errors and proceeds approximately twice as fast as it does at 25°C (Johnson and Weston, 1995). Thus, we used wildtype fish regenerating at 33°C as controls. To minimize differences in genetic background, we used heterozygous siblings as controls. In cases where siblings were not available, we used heterozygous fish of a similar genetic background.

Immunohistochemistry and in situ hybridization

Hematoxylin staining and whole-mount in situ hybridization were performed as described (Poss et al., 2000b). Six to 20 regenerates were examined for each time point. Immunohistochemistry on sectioned tissue was performed as described (Poss et al., 2000a, b), using the monoclonal ZNS-5 antibody (Johnson and Weston, 1995; Trevarrow et al., 1990). To generate antisense RNA probes for this study, we used a full-length 2.2-kb *sly1* cDNA (RZPD ID#WUSMp625H0347Q2), a full-length SG2NA cDNA (ESTfc02f06), a 4.9-kb TR#1 cDNA fragment (EST fc49f09), full-length *msxb* and *msxc* cDNAs (Akimenko et al., 1995), a 2.8-kb *left* cDNA fragment (Dorsky et al., 1999), a 1.8-kb *shh* cDNA (Laforest et al., 1998), a 2.8-kb *fgfr1* cDNA fragment (Poss et al., 2000b), and a 2.4-kb *wfgf* cDNA (Poss et al., 2000b). Simultaneous detection of *sly1* mRNA and PCNA antibody was performed as described (Nechiporuk and Keating, 2002). For BrdU incorporation experiments, fish ($n = 8$–10) were incubated in 50 μg/ml BrdU-containing water at a density of 5 fish per liter. For whole-mount detection of BrdU and phosphorylated histone-3 (H3P), fin regenerates were incubated in Carnoy's fixative (60% ethanol, 30% chloroform, and 10% acetic acid) overnight at 4°C. BrdU and H3P were detected as described (Nechiporuk and Keating, 2002).

Northern blot and RT-PCR expression analyses

For Northern blot analyses, 20–30 fin regenerates were collected directly into TRIzol Reagent (Invitrogen Life Technologies), processed using PowerGen 125 homogenizer (Fischer Scientific), and RNA was extracted according to the manufacturers protocol. Five micrograms of total RNA were separated on an agarose–formaldehyde gel, transferred to a Genescreen Plus (Dupont) nylon-based membrane. Blots were subjected to hybridization with a random-primed, ^{32}P-labeled probe according to the membrane manufacturers protocol. We used full-length *sly1* and *β-actin* cDNAs to generate hybridization probes.

For *sly1* RT-PCR, 1 μg of total RNA was reverse-transcribed with SuperScript II reverse-transcriptase (Invitrogen Life Technologies) by using oligo(dT) primer. RT reactions were carried out according to the manufacturers protocol. The resulting RT reactions were diluted fivefold, and 2 μl were used for RT-PCR. We used the following primers to detect *sly1* transcript: *sly1*-forward: 5′- ATTTGAACTTCATCTCCGCAATTTC-3′; *sly1*-reverse: 5′-GGTGAACAGGCTGTTACGAGCGTCT-3′. The resulting PCR product spans an intron and does not amplify genomic DNA. Amplification of *β-actin* was used in all experiments as a positive control to ensure the quality of mRNA.

TdT-mediated dUTP nick-end labeling (TUNEL)

Fin regenerates were fixed in 4% parafarmaldehyde in PBS (pH 7.4), embedded, and cryosectioned. Apoptotic cells were detected by using a commercially available In Situ Cell Death Detection Kit (Roche Molecular Biochemicals) according to the manufacturers protocols.

Genetic mapping and positional cloning

The *emm* gene was mapped to LG17 by centromere-linkage analysis (Johnson et al., 1996), using SSLP markers to genotype 35 EP progeny (Knapik et al., 1996; Shimoda et al., 1999). Fine genetic mapping was performed by using 1582 backcrossed progeny. Nonrecombinant marker Z22016 was used to screen a zebrafish P1 artificial chromosome (PAC) library (Amemiya et al., 1996). Resulting PAC clones were used to initiate a chromosomal walk. A

PAC contig was assembled by using recombination data generated from the PAC ends, as well as from EST clones that were previously mapped to the region by using radiation hybrid panels (Clark et al., 2001; Geisler et al., 1999). After defining the *emm* critical region, PAC clones were labeled and hybridized to day 1 and day 3 zebrafish regenerating fin cDNA libraries (R. Lee and S.L.J., unpublished data). To find the *emm* mutation, we compared *sly1* genomic sequences derived from *emm* and wildtype strains. The *emm* cDNA GenBank Accession No. is AY167023.

mRNA injections

The coding region of a wildtype *sly1* cDNA, or a *sly1* cDNA containing the 24-bp insertion was subcloned into the pCS2+ expression vector (Turner and Weintraub, 1994). For injections, RNA samples were prepared using the mMessage mMachine Kit (Ambion). Embryos were fertilized in vitro and injected at the one-cell stage as previously described (Westerfield, 2000). Pressure was adjusted to inject approximately 1 nl. Injected embryos were left to recover for 4–6 h at 25°C and then transferred to 33°C. Embryos were observed and scored daily. Wildtype embryos developed normally at 33°C; 87% (58 out of 62) developed a swim bladder by day 4 postfertilization.

Cell counting and statistical analysis

DAPI-, BrdU-, H3P-, and TUNEL-positive nuclei were counted from digitally captured images by using KS-300 software (Zeiss). Values were presented as means ± standard error of the mean (SEM). To compare means, we used Student's *t* test for data sets with either equal or unequal variances (Microsoft Excel 98 Data Analysis Tool package).

Electron microscopy

For electron microscopy, *emm* ($n = 3$) and wildtype ($n = 3$) fish were allowed to regenerate for 3 days at 25°C before a 6-h incubation at 33°C. Regenerates were collected and fixed in 2% glutaraldehyde and 0.03% picric acid in 100 mM cacodylate buffer overnight at 4°C. Tissue was postfixed in 2% osmium tetroxide in H_2O for 1 h at room temperature in the dark and then blocked in 1% uranyl acetate in H_2O for 30 min. Then tissue was dehydrated through an ethanol series, embedded in epon, and ultrasectioned for visualization on transmission electron microscope (JEOL-1200EX).

Results

A screen for temperature-sensitive fin regeneration mutants

Using an early pressure (EP) parthenogenetic scheme (Fig. 1A), we screened for adult fin regeneration mutants that showed inheritance consistent with a single gene defect. One of the isolated strains, which we named *emmental (emm)*, displayed a recessive block in fin regeneration at the restrictive temperature, 33°C, while regenerating normally at the permissive temperature, 25°C (Fig. 1B). To determine whether the *emm* gene is essential for embryonic development, we examined the effect of an embryonic temperature shift on survival. As predicted, the *emm* mutation was lethal at the restrictive temperature. *emm* individuals exhibited heterogeneous defects between 1 and 4 dpf, including dysmorphic heart, progressive pericardial edema, hooked tail, and shortened axes.

To define the regenerative block in *emm*, we performed gross morphological and histological analyses of fin regenerates. Wildtype fin regeneration at 33°C is reliable and proceeds approximately twice as fast as it does at 25°C (Johnson and Weston, 1995) (also see Materials and methods for more details). Wound healing and disorganization of intraray mesenchymal tissue during the first 12 h of regeneration were not affected in *emm* regenerates (Fig. 1B). However, during blastema formation, 18–24 h postamputation (hpa), we found that *emm* blastemal cells were not as densely packed as wildtype blastemal cells; this phenotype became more pronounced by 48 hpa (Fig. 1B). By this time point, most of the *emm* regenerates developed large acellular areas in the mesenchyme, often filled with clotted blood. The name *emmental* was derived from the resemblance of this phenotype to Swiss cheese. These observations suggest that the *emm* mutation blocks blastema formation.

To further define the critical period of regeneration affected by *emm*, we performed reciprocal temperature shift experiments (Fig. 1C). Upshift experiments (from 25 to 33°C) at any time point before the fin was fully regrown, blocked regeneration in mutants. In complementary downshift experiments, fish were preincubated for 24 h before fin amputation at 33°C and than shifted to 25°C during various time points. Mutants that were shifted to the permissive temperature before 18 hpa regenerated normally, whereas *emm* fish shifted after 18 hpa ceased to regenerate. These observations suggest that the critical period for *emm* begins after 18 hpa. Overall, we conclude that *emm* is not required during wound healing and tissue disorganization (0–12 hpa), but is essential for blastema formation and regenerative outgrowth (beyond 18 hpa).

Defective blastemal organization in emm mutants

Blastema formation is a crucial step in regeneration. In fact, the ability to form a blastema after limb or fin amputation is thought to distinguish regenerative teleosts and urodeles from less regenerative vertebrates (Brockes, 1997; Tsonis, 1996). Because *emm* mutants displayed a consistent disruption of blastema formation, we pursued fine characterization of the *emm* phenotype and positional cloning experiments to identify the mutated gene.

To determine the extent of the mesenchymal defect in

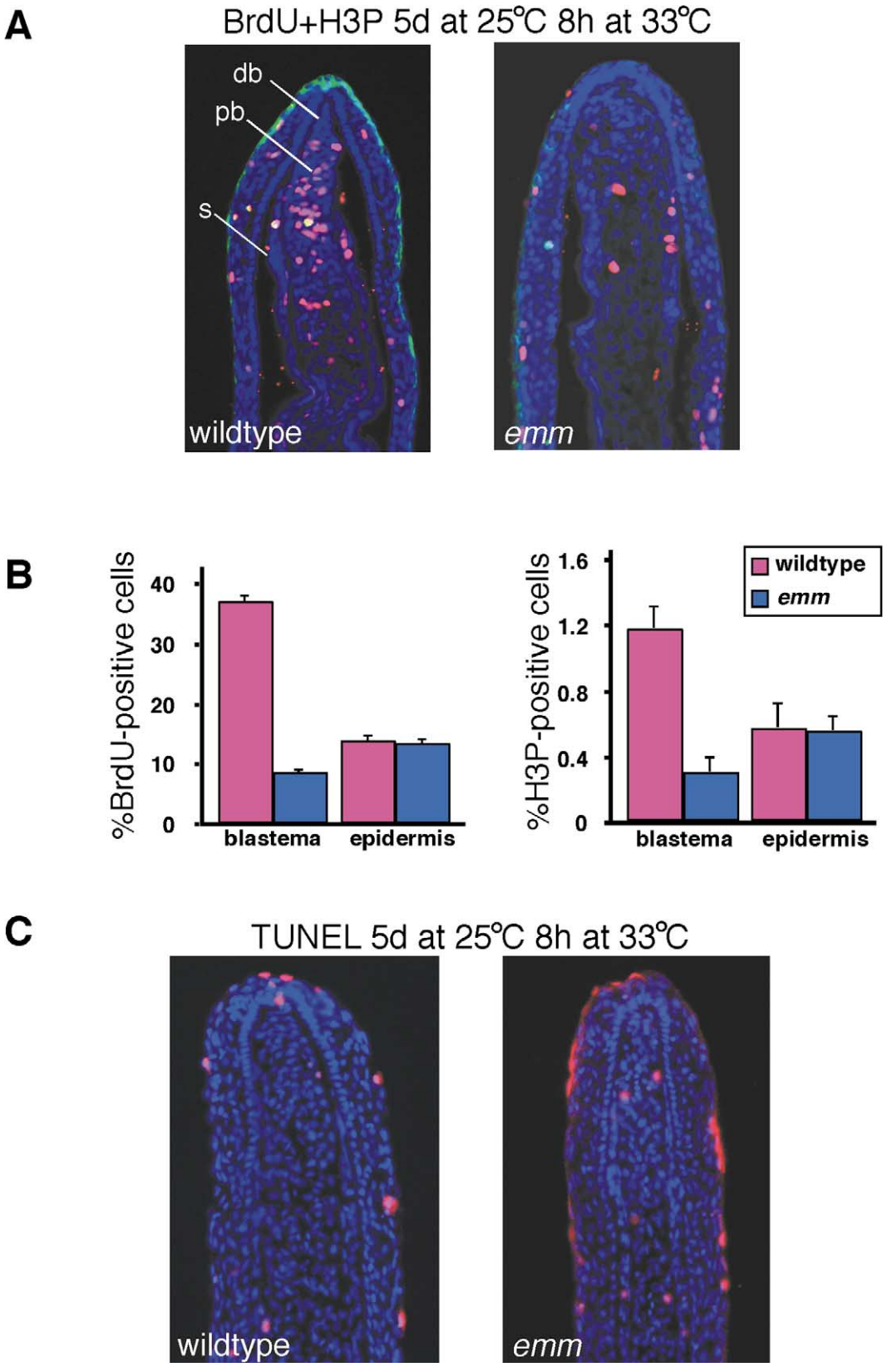

Fig. 3. Regenerative outgrowth is blocked in *emm* mutants. (A–C) Wildtype and *emm* fish were allowed to regenerate for 5 days at 25°C (~2.5 days at 33°C) before an 8-h incubation at 33°C. (A) Fluorescent longitudinal sections from wildtype (left) and *emm* (right) animals that were treated with BrdU during the final 2 h at 33°C. Regenerates have been processed for detection of BrdU (red) and H3P (green) and counterstained with DAPI (blue). Note that the number of BrdU- and H3P-positive cells in *emm* blastema is markedly reduced, indicating that *emm* is required for blastemal proliferation. (B) Indices of proliferation in the blastema and epidermis of wildtype and *emm* regenerates during regenerative outgrowth. The percentages of BrdU- and H3P-positive cells were obtained by counting 5,000–10,000 DAPI-positive nuclei from 10 sections from each of 4–5 immunostained regenerates. Note that the number of proliferating *emm* blastemal cells at each stage is greatly reduced, but that epidermal proliferation is unaffected. Results are shown as mean ± SEM (*, $P < 0.001$, *t* test). (C) Longitudinal sections processed

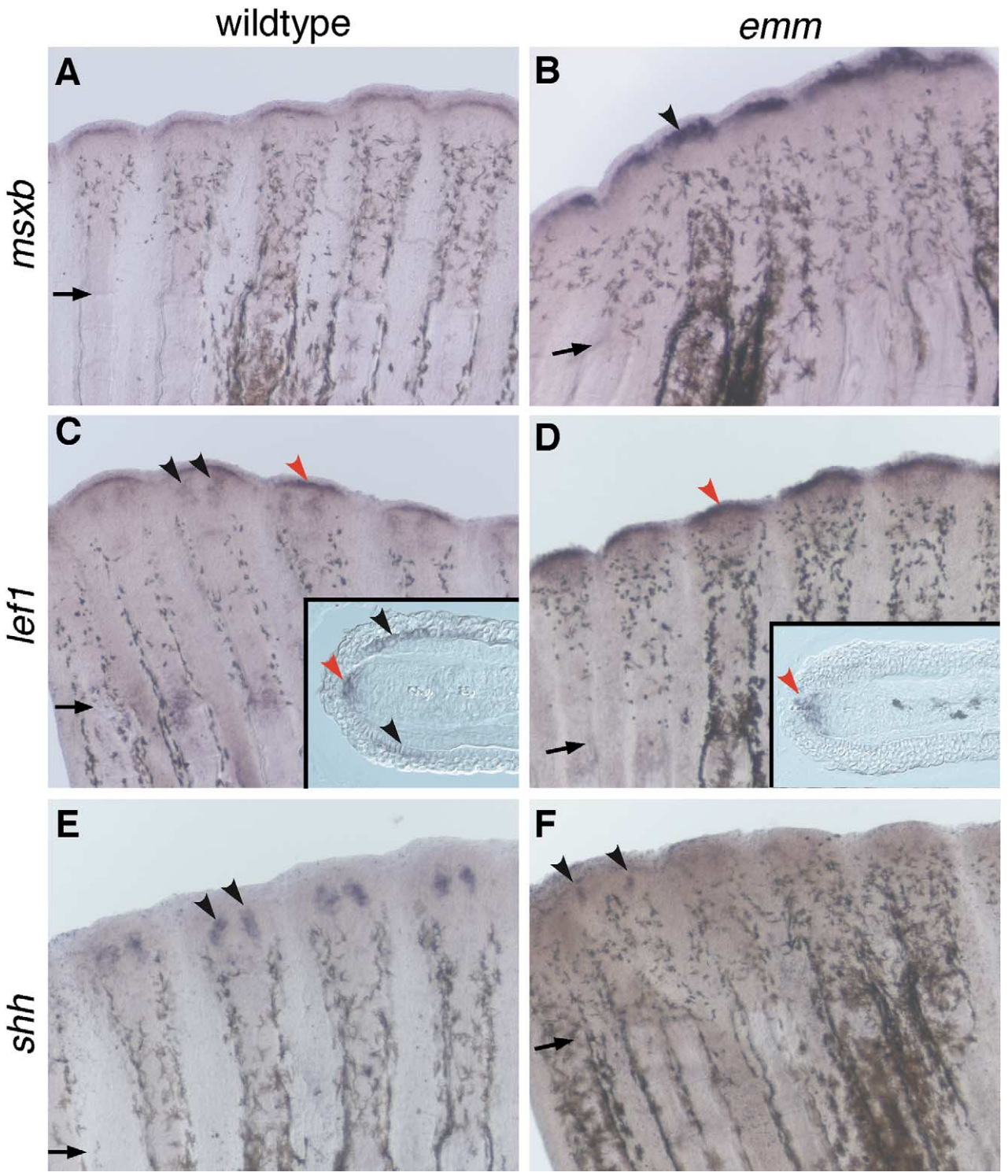

Fig. 4. Blastemal organization and epidermal gene expression are disrupted in *emm* fins during regenerative outgrowth. (A–F) Wildtype and *emm* fish were allowed to regenerate for 5 days at 25°C before an 8-h incubation at 33°C. Whole-mount in situ hybridizations of wildtype (A, C, and E) and *emm* (B, D, and F) fin regenerates, with the distal, regenerating end shown at the top. (A and B) *msxb* expression domain is expanded in *emm* regenerates (diffuse violet stain indicated by a black arrowhead; $n = 20$). (C and D) *lef1* expression is absent in the *emm* basal epidermis (black arrowheads), but persists in the distal blastema (red arrowheads; $n = 5$ and 9 for wildtype and *emm*, respectively). Insets show longitudinal sections obtained from the distal end of the corresponding whole-mount stained regenerates. Note the absence of *lef1* expression in the basal epidermis in *emm* regenerate. (E and F) Reduced *shh* expression in basal epidermal domain of *emm* regenerates (violet stain indicated by black arrows; $n = 5$ and 9 for wildtype and *emm*, respectively). Distal, regenerating end is at the top. Original magnification is 70× (insets, 180×).

for TUNEL (red) did not reveal any difference between wildtype and *emm* regenerates after 8-h heat treatment (*emm:* 3.28 ± 1.3% versus wt: 3.53 ± 0.48%; $P < 0.39$, *t* test; the percentages of TUNEL-positive cells were obtained by analyzing 3–7 sections from 4 wildtype and 6 *emm* regenerates). Abbreviations: db, distal blastema; pb, proximal blastema; s, scleroblasts. Distal, regenerating end is at the top. Original magnification in (A) and (C) is 180×.

emm regenerates, we examined expression of molecular markers. *msxb* is a homeodomain-containing transcriptional repressor, normally expressed in proliferating blastemal cells during blastema formation. *msxb* expression becomes limited to the distal blastema at the onset of regenerative outgrowth, 48 hpa (Akimenko et al., 1995; Poss et al., 2000b). *msxb* expression was indistinguishable from wildtype in *emm* regenerates during early blastema formation, 18–24 hpa (data not shown). However, *msxb* staining became diffuse at the onset of regenerative outgrowth (48 hpa), indicating defects in blastemal organization (Fig. 2A).

Sonic hedgehog (shh) is normally expressed in the basal layer of the wound epidermis, just distal to aligned scleroblasts 48 hpa (Laforest et al., 1998). Recently, Quint et al. (2002) demonstrated that ectopic expression of *shh* causes ray fusion. On the other hand, treatment of regenerating fins with cyclopamine, a specific Shh inhibitor, blocked fin regeneration and altered expression patterns of *shh* and its receptor *patched1 (ptc1)*. These observations suggested that Shh plays a patterning role during fin regeneration (Laforest et al., 1998; Quint et al., 2002). *shh* expression was undetectable in *emm* fin regenerates (Fig. 2B). Furthermore, scleroblasts were randomly dispersed throughout the regenerate, as assessed by Zns-5 antibody staining (Johnson and Weston, 1995) (Fig. 2B). These findings are consistent with the notion that *shh* is required for scleroblast alignment.

The reduced density of the *emm* blastema prompted us to examine proliferation indices in mutant regenerates. We studied DNA replication during blastema formation using bromodioxyuridine (BrdU) incorporation and mitoses using anti-phospho-histone-3 (H3P) antibody (Hendzel et al., 1997; Wei et al., 1999) (Fig. 2B and C). Proliferation levels during various stages of fin regeneration at 33°C have been previously characterized (Nechiporuk and Keating, 2002; Poss et al., 2002). Early mesenchymal proliferation (18 hpa) in *emm* fins was either comparable to, or slightly reduced from, that of controls (data not shown). The differences became more pronounced during blastema formation, 32 hpa (Fig. 2B and C). *emm* blastemal proliferation levels were ~30% lower than those of wildtype fish during blastema formation (32 hpa) as assessed by both BrdU and H3P staining (Fig. 2C; $P < 0.001$, Students *t* test). Interestingly, while blastemal proliferation levels were significantly reduced, epidermal proliferation levels remained normal (Fig. 2C; $P < 0.42$; *t* test). Thus, the *emm* mutation affects proliferating mesenchymal, but not epidermal, cells during blastema formation.

To determine whether programmed cell death contributed to reduced cellular density of the *emm* blastema, we performed TdT-mediated dUTP nick-end labeling (TUNEL) assays. We detected a small number of TUNEL-positive cells at 24 hpa. This number increased during mid- and late-blastema formation, 32 and 48 hpa, respectively (Fig. 3C, and data not shown; $P < 0.014$ for 32 hpa, *t* test). We did not detect any significant differences in labeling of the epidermis in *emm* and wildtype regenerates, although we saw consistent edge staining in *emm* and wildtype regenerates that might be explained by normal turnover of epidermal cells or by nonspecific labeling (Fig. 3C). Interestingly, colabeling of TUNEL-positive cells with Zns-5 antibody revealed few doubly labeled scleroblasts, demonstrating that differentiated scleroblasts were largely spared in *emm* fins (data not shown). From these observations, we conclude that loss of mesenchymal tissue during blastema formation in *emm* is attributed to decreased proliferation and increased programmed cell death in the blastema.

emm is required for regenerative outgrowth

We used temperature shift experiments to demonstrate that *emm* is also required during regenerative outgrowth (beyond 48 hpa). Because regenerative outgrowth was rapidly blocked following the temperature shift, we examined proliferation levels in outgrowing *emm* fin regenerates. Following a 5-day incubation at 25°C and 8-h incubation at 33°C, caudal fin regenerates were examined for proliferation levels by BrdU incorporation and H3P staining (Fig. 3A and B). We found that *emm* blastemal proliferation was reduced by ~4.5 times relative to the wildtype controls when assayed by both BrdU incorporation and H3P labeling (Fig. 3B; $P \ll 0.001$, *t* test). However, epidermal proliferation levels remained normal at both stages (Fig. 3B; $P < 0.36$; *t* test). We failed to detect any difference in TUNEL staining between *emm* and wildtype control fins, indicating that short heat treatment did not induce programmed cell death (Fig. 3C; $P < 0.39$; *t* test). These data suggest that the *emm* mutation affects proliferation of blastema, but not wound epidermis, during regenerative outgrowth.

Recently, we found that the blastema is subdivided into two zones during regenerative outgrowth: a nonproliferative, *msxb*-positive distal zone, and a highly proliferative, PCNA-positive, *msxb*-negative proximal zone. We asked whether *emm* is required for maintenance of blastemal zones during regenerative outgrowth. In situ hybridizations with *msxb* probe demonstrated that the distal blastema (DB) was expanded in 50% of all *emm* fins examined ($n = 20$) after the 8-h heat treatment (Fig. 4A and B). This observation was confirmed by other markers specific to the DB, including *msxc* and *lef1* (Fig. 4C and D, and data not shown). Even after a brief, 2-h heat treatment, we saw an expansion of *msxb* domain in a small number of fins (data not shown). As expected based on BrdU and H3P analyses, PCNA antibody staining was markedly reduced in the proximal blastema (PB) of *emm* fins (data not shown).

Previous studies indicate that Fgf signaling is required for regenerative outgrowth, during which it maintains *msxb* and *msxc* expression (Poss et al., 2000b). At least one Fgf family member, wound *fgf (wfgf)*, is expressed in the distal part of the wound epidermis immediately adjacent to the distal blastema, whereas *fgfr1* is expressed in two distinct domains, the distal blastema and the lateral basal epidermis (Poss et al., 2000b). Because the *emm* mutation inhibited

regenerative outgrowth, we examined expression of *wfgf* and *fgfr1* in *emm* regenerates. The intensity and distribution of epidermal *wfgf* and blastemal *fgfr1* signal appeared to be normal in *emm* fins, suggesting that the expression of Fgf members is not affected ($n = 15$ and 5 for *wfgf* and *fgfr1*, respectively; data not shown). However, we failed to detect any epidermal *fgfr1* expression in *emm* fins. The expression of two other epidermal markers, *lef1* and *shh*, was also significantly reduced (Fig. 4C–F). *lef1* was expressed in 43% of all *emm* rays examined (67 rays examined from 9 regenerates), compared with 92% rays of wild type rays (37 rays examined from 5 regenerates). Similarly, *shh* was expressed in 66% of all *emm* rays examined (65 rays examined from 9 regenerates) compared with 80% in wildtype (40 rays examined from 5 regenerates). Interestingly, similar decreases in *lef1* and *shh* epidermal expression were observed during the regenerative block caused by treatment with SU5402 (Poss et al., 2000b), a specific Fgfr1 inhibitor (Mohammadi et al., 1997). We interpret the reduced epidermal expression of *fgfr1*, *lef1*, and *shh* to be an indirect consequence of disrupted epithelial–mesenchymal interactions during the regenerative block. Overall, these data indicate that *emm* is required for blastemal organization during regenerative outgrowth in addition to its requirement during blastema formation.

Positional cloning of the emm gene

To reveal the identity of *emm*, we used a positional cloning approach. *emm* was mapped to linkage group (LG) 17 by half-tetrad analysis (Johnson et al., 1995, 1996) by using simple sequence length polymorphisms (SSLP) (Knapik et al., 1996; Shimoda et al., 1999). SSLP marker Z22016 was nonrecombinant with *emm* in 1582 backcrossed individuals (Fig. 5A). We initiated a chromosome walk from this marker using P1 artificial chromosome (PAC) clones. We developed single strand conformation polymorphism (SSCP) markers from the ends of PAC clones and used them to identify the critical, nonrecombinant region around *emm*. As shown on Fig. 5A, PAC clones 67d8, 234g15, 178g23, and 142b24 defined a physical interval of approximately 220 kb that contained the *emm* gene.

To identify expressed sequences in the critical region, we first used PAC clones to screen 1- and 3-day zebrafish fin regeneration cDNA libraries (R. Lee and S.L.J, unpublished data). We obtained six positive clones, from which five represented an orthologue of yeast *sly1* (for suppressor of loss of *YPT1* function) and one clone represented an orthologue of SG2NA (S to G2 Nuclear Antigen). Subsequently, the PAC contig was sequenced and annotated as a collaborative effort with The Sanger Institute (www.sanger.ac.uk/Projects/D_rerio/). Analysis of the sequencing data revealed that the critical region is ~285 kb and contains seven transcripts (Fig. 5A). The entire region is syntenic to the ~900-kb interval on human chromosome 14q12, which also contains seven homologous transcripts. In addition to *sly1* (human designation *RA410*) and *SG2NA*, *pie* (homolog of the Drosophila pineapple eye, human designation *FLJ20333*), *COL12A1*, (homolog of the human cochlin), *AP4S1* (adaptor-related protein complex 4, sigma 1), *TR#1* (unknown gene, designated here transcript #1), and *TR#2* (unknown gene, designated here transcript #2) transcripts were localized to the critical region. Using genomic sequence data, we developed SSCP markers immediately distal to the *pie* and *TR#2* transcripts, but they were nonrecombinant in our backcross panel. We analyzed these transcripts for expression in the regenerating fins during blastema formation and outgrowth by RT-PCR and either in situ hybridization or Northern blot analysis. We detected expression of *sly1*, *SG2NA*, and *AP4S1* during both blastema formation and regenerative outgrowth stages of fin regeneration, whereas *pie*, *COL12A1*, and *TR#2* were primarily expressed during one of two stages. The remaining transcript in the critical region, *TR#1*, was not expressed in regenerating fins.

We sequenced all transcripts localized to the critical region, except *TR#1*. Initial analysis of RT-PCR products from mutants and wildtype controls revealed that *sly1* cDNA from *emm* individuals contained a 24-bp insertion at position 459 (Fig. 5B). Further analyses showed the pres-

Fig. 5. Positional cloning of the *emm* gene. (A) Genetic and physical map of LG17 containing the *emm* gene (top, linkage map; middle, transcript map; bottom, PAC map). Initial genetic mapping placed *emm* between SSLP markers Z9818 and Z1278, whereas SSLP marker Z22016 was nonrecombinant. A chromosomal walk was initiated from Z22016 by using PAC clones. SSCP markers, 67d8t7 and 142b24sp6, were generated from the ends of these clones and used for fine recombination mapping. The number of recombinants between *emm* and each SSCP marker among 1582 meioses are shown in parentheses above the genetic map. We identified potential transcribed sequences in the critical region by hybridizing PAC clones to gridded cDNA libraries as well as using conserved synteny with human genomic sequence. In addition, zebrafish transcript sequences were obtained from the annotated version of the zebrafish genome at the The Sanger Institute (www.sanger.ac.uk/Projects/D_rerio/) and from EST assemblies (designated here as WZ) at Washington University, http://www.genetics.wustl.edu/sjlab/RW/ (R. Waterman and S.L.J., unpublished observations). (B) Genomic (top) and cDNA sequence (bottom) of the *sly1* mutated region from *emm* and wildtype individuals. Initial sequencing analysis identified a 24-bp insertion (red) in cDNA derived from *emm* individuals. Further sequence analyses revealed the presence of two transcripts, one containing a 24-bp insertion and a second containing a 9-bp deletion. Sequence analyses of genomic DNA from *emm* mutants revealed a T-to-A transversion (red) in a consensus donor splice site (underlined) that led to generation of two aberrant transcripts from two cryptic splice sites (black arrowheads). (C) RT-PCR analyses from *emm* and various wildtype strains at 25°C (left) and 33°C (right). Note the presence of two aberrant products in *emm* individuals at both temperatures, indicating that mutant transcripts are spliced at both temperatures; these products were absent in all wildtype zebrafish strains examined, including the original mutagenized, inbred SJD strain. (D) Multiple species alignment of the *sly1* region containing the mutation. Note the very high conservation of this domain among vertebrates.

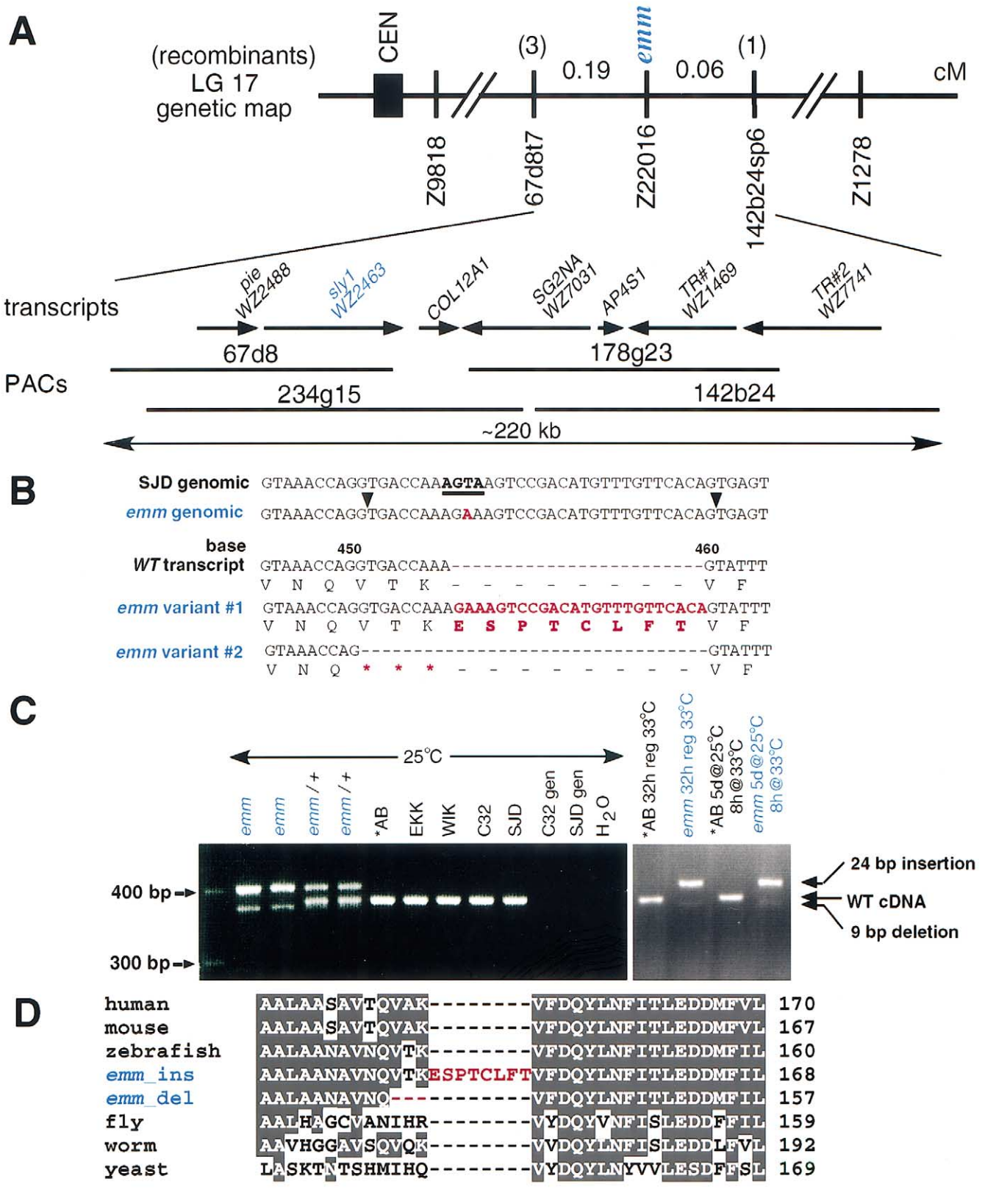
A
(recombinants)
LG 17
genetic map
CEN
(3)
0.19
emm
0.06
(1)
cM
Z9818
67d8t7
Z22016
142b24sp6
Z1278
transcripts
pie
WZ2488
sly1
WZ2463
COL12A1
SG2NA
WZ7031
AP4S1
TR#1
WZ1469
TR#2
WZ7741
PACs
67d8
178g23
234g15
142b24
~220 kb
B
SJD genomic GTAAACCAGGTGACCAAAGTAAGTCCGACATGTTTGTTCACAGTGAGT
emm genomic GTAAACCAGGTGACCAAAGAAAGTCCGACATGTTTGTTCACAGTGAGT
base
450
460
WT transcript GTAAACCAGGTGACCAAA----------GTATTT
V N Q V T K - - - - - - - - - V F
emm variant #1 GTAAACCAGGTGACCAAAGAAAGTCCGACATGTTTGTTCACAGTATTT
V N Q V T K E S P T C L F T V F
emm variant #2 GTAAACCAG----------GTATTT
V N Q * * * - - - - - - - - - V F
C
25°C
emm
emm
emm / +
emm / +
*AB
EKK
WIK
C32
SJD
C32 gen
SJD gen
H2O
*AB 32h reg 33°C
emm 32h reg 33°C
*AB 5d@25°C
8h@33°C
emm 5d@25°C
8h@33°C
400 bp
300 bp
24 bp insertion
WT cDNA
9 bp deletion
D
human AALAASAVTQVAK--------VFDQYLNFITLEDDMFVL 170
mouse AALAASAVTQVAK--------VFDQYLNFITLEDDMFVL 167
zebrafish AALAANAVNQVTK--------VFDQYLNFITLEDDMFIL 160
emm_ins AALAANAVNQVTKESPTCLFTVFDQYLNFITLEDDMFIL 168
emm_del AALAANAVNQ----------VFDQYLNFITLEDDMFIL 157
fly AALHAGCVANIHR--------VYDQYVNFISLEDDFFIL 159
worm AAVHGGAVSQVQK--------VVDQYLNFISLEDDLFVL 192
yeast LASKTNTSHMIHQ--------VYDQYLNYVVLESDFFSL 169

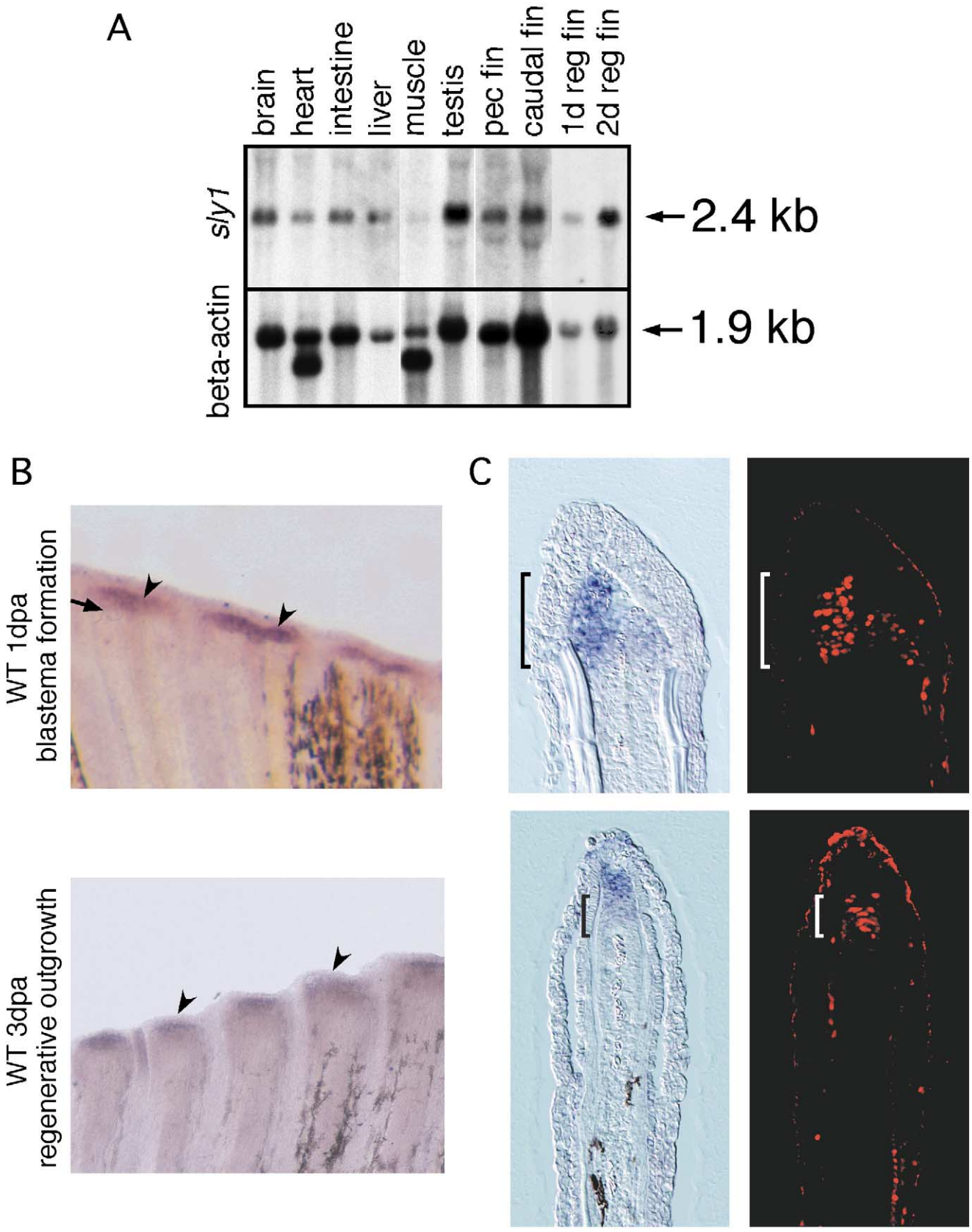

Fig. 6. *sly1* is induced in blastemal cells during regeneration. (A) Northern analysis of *sly1* distribution in somatic tissues and intact and regenerating caudal fins. *sly1* is widely expressed, with the highest expression levels in testis and liver. *sly1* levels are upregulated twofold during blastema formation and fourfold during regenerative outgrowth, as determined by phosphoimaging. Blots were also probed for *β-actin* to indicate the amounts of RNA loaded. (B) Whole-mount in situ hybridizations of *sly1* during blastema formation (top; 1 dpa) and regenerative outgrowth (bottom; 3 dpa) in wildtype fins. *sly1* is upregulated in the newly formed blastema, and is maintained during outgrowth (violet stain; arrowheads). (C) Longitudinal sections of 1- (top) and 3-day regenerates (bottom) constained for *sly1* antisense RNA and PCNA protein (red). Note that *sly1* is upregulated in proliferative cells during blastema formation, but its expression is mostly restricted to nonproliferative distal blastemal cells during outgrowth. The distal, regenerating end is at top. Original magnification: 70x in (A) and 180x in (B).

Table 1
Overexpression of *sly1* partially rescues early embryonic lethality of *emm*[a]

RNA	200 ug/μl			75 ug/μl		
	n[b]	Swim bladder present (%)	Swim bladder absent (%)	*n*	Swim bladder present (%)	Swim bladder absent (%)
EGFP	49	4	96	83	0	100
$sly1^{+}$	65	34 ($P < 0.023$)[c]	66	160	13 ($P < 0.0012$)	87
$sly1^{-/-}$	56	9 ($P < 0.12$)	91	52	4 ($P < 0.16$)	96

[a] Embryos were collected from six and five homozygous crosses for 200 and 75 ug/μl RNA injection regiments, respectively. After injections, embryos were allowed to recover for 4-6 h at 25°C and then transferred to 33°C. Embryos were scored for the presence or absence of swim bladders at 4 days postfertilization.

[b] Total number of embryos examined.

[c] The percentages of embryos that develop swim bladders from EGFP mRNA injections were compared with the percentages derived from $sly1^{+}$ and $sly1^{-/-}$ RNA injections using Mann–Whitney test.

ence of two RT-PCR products in *emm* individuals. The larger cDNA product contained a 24-bp insertion (variant#1 on Fig. 5B and C), whereas the smaller, less intense product contained a 9-bp deletion (variant#2 on Fig. 5B and C). RT-PCR of heterozygous individuals revealed the presence of three products, variants 1 and 2, and the wildtype transcript. None of the wildtype strains examined, including the original inbred, mutagenized SJD strain, contained the aberrant products (Fig. 5C). By sequencing mutant and wildtype genomic DNA, we identified a single T-to-A transversion in the splice donor site that led to the generation of two mutant transcripts from two cryptic splice sites. These sites are shown in Fig. 5B (arrowheads). Both aberrant transcripts were present at 25°C (Fig. 5C, left) and 33°C (Fig. 5C, right) in mutants, indicating that this mutation does not cause temperature-dependent splicing.

Sly1 belongs to the Sec1 (Sec for secretion) family of proteins involved in synaptic transmission and general secretion. Previous studies demonstrated that members of the Sec1 family are essential for vesicle trafficking and protein secretion. Analysis of null and TS mutations in yeast demonstrated that sly1 is involved in protein and vesicle transport between ER and Golgi (Dascher et al., 1991; Mizuta and Warner, 1994). More recently, Sly1 has been shown to bind ER syntaxins, suggesting that it is required for Golgi-to-ER retrograde transport (Yamaguchi et al., 2002). The absence of Sly1 function in yeast produced severe defects in protein secretion (Mizuta and Warner, 1994). Zebrafish sly1 is 33, 58, and 88% identical to the yeast, fly, and human Sly1 homologues, respectively, at the amino acid level. The *emm* mutation (allele designation $sly1^{zp2}$) alters a Sec1 domain of Sly1 that is highly conserved among all vertebrate species, and semiconserved in *D. melanogaster*, *C. elegans*, and *S. cerevisiae* (Fig. 5D).

To confirm that *sly1* is the *emm* gene, we carried out embryonic rescue experiments. As mentioned above, *emm* is embryonic-lethal at the restrictive temperature. We injected mRNA encoding wildtype (sly^{+}) and mutant ($sly1^{-/-}$, containing 24-bp insertion) transcripts, into one-cell-stage homozygous *emm* embryos at two concentrations, 75 and 200 ng/μl (Table 1). After injections, embryos were transferred to 33°C. We scored the injected embryos for the absence or presence of a swim bladder at 4 dpf, because *emm* mutant embryos consistently fail to produce swim bladders at this temperature [only 6 out of 166 (4%) *emm* embryos examined developed swim bladders; data not shown]. As controls, we examined embryos injected with an EGFP mRNA. At 33°C, most wildtype embryos did not exhibit embryonic defects and developed normally until the swimming stage (58 of 64 embryos examined, or 87%, developed swim bladders 4 dpf; data not shown). However, fewer than 9% of *emm* embryos injected with either EGFP or $sly1^{-/-}$ mRNA developed swim bladder (Table 1). In contrast, 34% ($P < 0.023$; Mann–Whitney test) and 13% ($P < 0.0012$) of all embryos that were injected with 200 or 75 ng/μl $sly1^{+}$ mRNA, respectively, were able to swim at 4 dpf. We conclude that *sly1* overexpression partially rescues embryonic lethality of *emm* mutants. Thus, our linkage, mutational, and mRNA rescue data all indicate that *sly1* is the *emm* gene. We will refer to *emm* animals hereafter as *sly1* mutants.

sly1 expression is induced in blastemal cells

We next analyzed expression of *sly1* in regenerating zebrafish fins. Northern blot analyses revealed that *sly1* was widely expressed in adult zebrafish tissues, with the highest expression in liver and testis (Fig. 6A). Interestingly, adult male *emm* mutant fish showed reduced mating efficacy, and often were depleted of sperm. A basal level of *sly1* transcription was maintained in the intact caudal and pectoral fins (Fig. 6A). However, levels of *sly1* mRNA increased two-to fourfold during fin regeneration. We did not detect any differences in the levels of *sly1* transcript in wildtype and *sly1* regenerates at 33°C (Fig. 5C). In situ hybridization experiments did not detect *sly1* transcripts during wound healing (0–12 hpa), but they were detected in proliferating blastemal cells during blastema formation (18–48 hpa; Fig. 6B, and data not shown). During regenerative outgrowth, the highest levels of *sly1* were detected in the non-, or slowly proliferating distal blastema, with lower levels in the proximal blastema. These data indicate that *sly1* is upregu-

lated in blastemal cells during blastema formation and regenerative outgrowth, an observation that helps to explain the *sly1* phenotype.

ER stress in emm blastema

Conditions that compromise ER–Golgi transport promote accumulation of unfolded proteins in the rough ER lumen, a phenomenon known as ER stress (Ferri and Kroemer, 2001). We hypothesized that a block in vesicular transport caused by the *sly1* mutation might induce ER stress. To test this hypothesis, we analyzed mutant and wildtype blastemal cells using transmission electron microscopy (TEM). To ensure that subcellular changes were induced specifically by the *sly1* mutation, we took advantage of the conditional nature of the mutation. Following caudal fin amputation, fish were incubated at the permissive temperature for 3 days before shifting to the restrictive temperature for 6 h. At this point, fin regenerates were collected and processed for TEM. TEM revealed that control blastemal cells had large nuclei with pronounced nucleoli, abundant polyribosomes, rough ER, and mitochondria. These are typical characteristics of highly proliferative cells (Fig. 7). We found that the rough ER lumen was dramatically swollen in *sly1* mutant blastemal cells (Fig. 7), a likely indication of abnormal accumulation of protein in the ER. This observation is consistent with ER stress (Bauer et al., 2002).

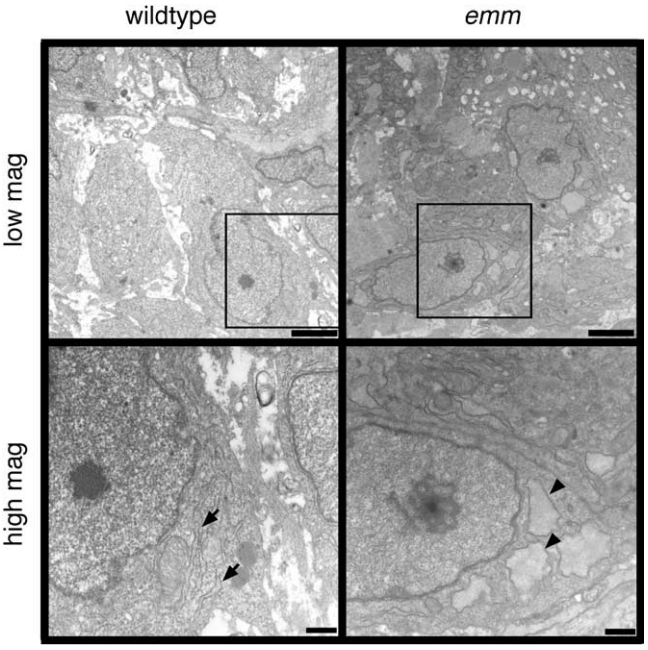

Fig. 7. ER stress in *sly1* blastemal cells. (A) Wildtype and *sly1* blastemal cells were analyzed by transmission electron microscopy (TEM). After fin amputation, *sly1* and wildtype fish were incubated at the permissive temperature for 3 days before transfer to the restrictive temperature. Regenerates were collected 6 h later and processed for TEM. Low (top) and high (bottom) magnification micrographs of blastemal cells from wildtype (left) and *emm* (right) regenerates are shown. High magnification images were taken from the areas indicated by rectangles. Blastemal cells exhibit abundant rough ER, mitochondria, and pronounced nucleoli, all characteristics of rapidly proliferating cells. Note presence of abnormally swollen rough ER in *emm* blastemal cells (arrowheads), suggesting ER stress. Scale bars: top, 2 μm; bottom, 0.5 μm.

Discussion

In this study, we used a classical genetic approach to identify genes required for vertebrate regeneration. One of the TS strains identified in this screen, *emm*, displayed problems with blastemal organization during blastema formation and regenerative outgrowth. Using positional cloning, we discovered that the *emm* temperature-sensitive defect is caused by a mutation in the *sly1* gene. Evidence indicating that *sly1* is the *emm* gene include: (1) genetic linkage of *emm* to the 0.25 cM region containing *sly1;* (2) absence of mutations in other genes that mapped to the critical region; (3) identification of a splice site mutation in the *sly1* gene that alters the *sly1* transcript in *emm* individuals; (4) absence of the mutation in all common zebrafish strains, including the original, inbred SJD strain used in mutagenesis, indicating that this mutation is not a common polymorphism; (5) rescue by *sly1* mRNA of *emm* embryonic lethality; (6) expression data demonstrating that the timing and location of *sly1* expression is consistent with the mutant phenotype; (7) EM data indicating that *sly1* mutant blastemal cells develop ER stress, consistent with the known involvement of sly1 in ER to Golgi vesicle transport. This study, together with the positional cloning of a second mutation that causes an adult regeneration defect (Poss et al., 2002), demonstrate that standard genetic approaches can be used to find genes essential for fin regeneration in zebrafish.

Mechanism of sly1 mutant pathology

A number of previous studies have indicated that sly1 has an essential cellular function, mediating vesicular transport and protein secretion (Dascher et al., 1991; Mizuta and Warner, 1994; Yamaguchi et al., 2002). The requirement for sly1 may be enhanced in regenerating blastemal cells, which are involved in intense proliferation and cell-to-cell signaling. In support of this idea, prolonged heat-inactivation of sly1 is lethal in blastemal cells during regeneration. Furthermore, a 4- to 8-day heat treatment of *sly1* fish leads to 75% lethality (data not shown), indicating that sly1 is essential for adult physiology and survival. However, gross observations of morbidity in *emm* fish cannot be observed until 3 days after development of the regenerative block, and thus are probably not the basis of the regeneration defect.

What is the mechanism of *sly1* pathology in regenerating fins? We found that the *sly1* phenotype correlated well with

blastemal expression of *sly1* mRNA during regeneration, as *sly1* mutants fail to form mature blastema during blastema formation. At the subcellular level, *sly1* mutants develop ER stress. It has been shown that ER stress is associated with activation of the caspase cascade and programmed cell death (Nakagawa and Yuan, 2000; Nakagawa et al., 2000; Yoneda et al., 2001; Zinszner et al., 1998). Prolonged heat treatment of *sly1* regenerates during blastema formation induced apoptosis in the blastemal cells. These observations indicate that loss of mesenchymal tissue and subsequent regeneration failure during blastema formation in *sly1* mutants can be attributed, at least in part, to reduced blastemal proliferation and programmed cell death.

Interestingly, brief heat treatments employed to study the role of Sly1 during regenerative outgrowth did not induce cell death, but still blocked regeneration. Sly1 inactivation led to a rapid regenerative block, characterized by down-regulation of markers potentially involved in differentiation and patterning, such as *shh*, *lef1*, and *fgfr1*. This regenerative block was also marked by the rapid reduction of blastemal proliferation and disruption of blastemal zones.

Previous studies demonstrated that Fgf signaling is necessary to induce *msxb/c* expression during blastema formation, and maintain expression during outgrowth. However, both *msxb* and *msxc* were induced in *sly1* regenerates during blastema formation, and *msxb/c* expression was maintained, albeit in a diffused pattern, after heat- shock. Thus, it is unlikely that this block is due to a specific disruption in the trafficking or secretion of Fgf signaling pathway members. The diffuse *msxb/c* staining might represent an expansion of the distal blastemal domain. Correspondingly, we observed decreased proximal blastemal PCNA staining, suggesting a decrease in function of this compartment. We can provide two interpretations of these observations. First, *sly1* is expressed at low levels in rapidly proliferating, proximal blastemal cells that may have an enhanced requirement for protein and vesicular trafficking. Sly1 inactivation blocks proliferation, and might lead to a compensatory expansion of the nonproliferative, distal blastemal domain.

Alternatively, the block in proliferation during regenerative outgrowth may be an indirect consequence of the disruption of the distal blastema. We have previously suggested that distal blastemal cells represent a pool of progenitors (Poss et al., 2002, 2003). In this model, the *msxb/c*-positive distal blastemal compartment is maintained by the expression of growth factors in the apical epidermis, potentially by *wfgf*. During regenerative outgrowth, distal blastemal cells slowly divide and their progeny enter the proliferative zone. Intense proliferation in the proximal blastema drives regenerative outgrowth, while blastemal cells exit the cell cycle and differentiate and/or pattern under the influence of Shh and other factors. Thus, a perturbation of the distal blastema might indirectly affect proliferation levels in the proximal blastema disrupting the supply of blastemal precursors. Interestingly, expansion of the distal blastemal zone in *sly1* mutants could reveal a sly1-dependent mechanism that suppresses expression of *msxb/c* from more proximal blastemal regions. Such a mechanism may include processing of a signaling molecule(s) that repress its expression. We have previously suggested that upregulation of *msxb* inhibits proliferation in the distal blastema. Therefore, the proliferative decrease in *emm* blastema may be a consequence of *msxb* expansion into more proximal regions of the blastema.

Regeneration and stress-response

It is believed that the blastema comprises a population of progenitor cells that undergo proliferation, differentiation, and morphogenesis to gives rise to missing structures. In other words, blastemal cells possess stem cell-like properties. Recent study identified more than 200 genes that are commonly enriched in various stem cells types (Ramalho-Santos et al., 2002). A significant number of these belonged to the so-called stress-response genes, including DNA repair, protein folding, vesicular trafficking, ubiquitin pathway, and detoxifier system genes. The reason for this upregulation is unknown, but one may speculate that DNA replication and protein folding require stringent control, given the potential for amplification of mutations in stem cell progeny. Alternatively, this observation may reveal a mechanism that protects stem cells from the deleterious effects of oxidative stress. Interestingly, the human *sly1* orthologue, *RA410*, was initially isolated as an immediate early gene in the screen for factors that participate in the ischemia-related stress response (Matsuo et al., 1997). Therefore, it is likely that a certain number of stress-response genes are upregulated in the regenerating blastema. In support of this, we have found that a number of stress-response genes are induced in regenerating zebrafish fins, including hsp90, 47-kDa heat-shock protein, cytochrome oxidase III, and 60Sribosomal protein (http://www.genetics.wustl.edu/sjlab/RW/; R. Waterman and S.L.J., unpublished observations). Thus, we expect that a certain percentage of fin regeneration mutants will harbor mutations in stress-response genes.

We also anticipate that mutagenesis screens, such as the one described here, will generate additional conditional, temperature-sensitive mutations in basic subcellular processes. Such mutants represent new reagents for studying gene function in the context of the embryonic and adult organism. The majority of null or hypomorphic mutations that have been isolated during zebrafish embryonic screens define the earliest requirements for disrupted genes. The availability of a TS allele, by contrast, allows disruption of gene function during later stages of development simply by changing the water temperature. Accordingly, we predict that the TS *sly1* zebrafish strain described here will be a useful reagent for studying such processes as vesicular trafficking, protein secretion, and apoptosis in vertebrates.

Acknowledgments

We are grateful to the members of Stephen Johnson's lab for technical advice during the mutagenesis screen. We thank Jennifer Sheppard, Janet Finney, Ann Hillam, Lindsay Wilson, Angela Sanchez, and Soo Kim for excellent fish care. We also thank the members of the Electron Microscopy core facilities at the Department of Cell Biology, Harvard Medical School for help with transmission electron microscopy. K.D.P. was supported by a postdoctoral fellowship from the Helen Hay Whitney Foundation. S.L.J. was supported by NIH PO1 Grant HD39952.

References

Akimenko, M.A., Johnson, S.L., Westerfield, M., Ekker, M., 1995. Differential induction of four msx homeobox genes during fin development and regeneration in zebrafish. Development 121, 347–357.

Amemiya, C.T., Ota, T., Litman, G., 1996. Construction of P1 artificial chromosome (PAC) libraries from lower vertebrates. Birren, B.W., Lai, E. (Eds.), in Nonmammalian Genomic Analysis, Academic Press, San-Diego, pp. 223–256.

Bauer, J., Bradl, M., Klein, M., Leisser, M., Deckwerth, T.L., Wekerle, H., Lassmann, H., 2002. Endoplasmic reticulum stress in PLP-overexpressing transgenic rats: gray matter oligodendrocytes are more vulnerable than white matter oligodendrocytes. J. Neuropathol. Exp. Neurol. 61, 12–22.

Becerra, J., Junqueira, L.C., Bechara, I.J., Montes, G.S., 1996. Regeneration of fin rays in teleosts: a histochemical, radioautographic, and ultrastructural study. Arch. Histol. Cytol. 59, 15–35.

Becerra, J., Montes, G.S., Bexiga, S.R., Junqueira, L.C., 1983. Structure of the tail fin in teleosts. Cell Tissue Res. 230, 127–137.

Brockes, J.P., 1997. Amphibian limb regeneration: rebuilding a complex structure. Science 276, 81–87.

Clark, M.D., Hennig, S., Herwig, R., Clifton, S.W., Marra, M.A., Lehrach, H., Johnson, S.L., Groupt, W., 2001. An oligonucleotide fingerprint normalized and expressed sequence tag characterized zebrafish cDNA library. Genome Res. 11, 1594–1602.

Dascher, C., Ossig, R., Gallwitz, D., Schmitt, H.D., 1991. Identification and structure of four yeast genes (SLY) that are able to suppress the functional loss of YPT1, a member of the RAS superfamily. Mol. Cell. Biol. 11, 872–885.

Dorsky, R.I., Snyder, A., Cretekos, C.J., Grunwald, D.J., Geisler, R., Haffter, P., Moon, R.T., Raible, D.W., 1999. Maternal and embryonic expression of zebrafish lef1. Mech. Dev. 86, 147–150.

Driever, W., Solnica-Krezel, L., Schier, A.F., Neuhauss, S.C., Malicki, J., Stemple, D.L., Stainier, D.Y., Zwartkruis, F., Abdelilah, S., Rangini, Z., Belak, J., Boggs, C., 1996. A genetic screen for mutations affecting embryogenesis in zebrafish. Development 123, 37–46.

Ferri, K.F., Kroemer, G., 2001. Organelle-specific initiation of cell death pathways. Nat. Cell Biol. 3, E255–E263.

Geisler, R., Rauch, G.J., Baier, H., van Bebber, F., Brobeta, L., Dekens, M.P., Finger, K., Fricke, C., Gates, M.A., Geiger, H., Geiger-Rudolph, S., Gilmour, D., Glaser, S., Gnugge, L., Habeck, H., Hingst, K., Holley, S., Keenan, J., Kirn, A., Knaut, H., Lashkari, D., Maderspacher, F., Martyn, U., Neuhauss, S., Haffter, P., et al., 1999. A radiation hybrid map of the zebrafish genome. Nat. Genet. 23, 86–89.

Geraudie, J., Singer, M., 1992. The fish fin regenerate. Monogr. Dev. Biol. 23, 62–72.

Golling, G., Amsterdam, A., Sun, Z., Antonelli, M., Maldonado, E., Chen, W., Burgess, S., Haldi, M., Artzt, K., Farrington, S., Lin, S.Y., Nissen, R.M., Hopkins, N., 2002. Insertional mutagenesis in zebrafish rapidly identifies genes essential for early vertebrate development. Nat. Genet. 31, 135–140.

Haffter, P., Granato, M., Brand, M., Mullins, M.C., Hammerschmidt, M., Kane, D.A., Odenthal, J., van Eeden, F.J., Jiang, Y.J., Heisenberg, C.P., Kelsh, R.N., Furutani-Seiki, M., Vogelsang, E., Beuchle, D., Schach, U., Fabian, C., Nusslein-Volhard, C., 1996. The identification of genes with unique and essential functions in the development of the zebrafish, Danio rerio. Development 123, 1–36.

Halachmi, N., Lev, Z., 1996. The Sec1 family: a novel family of proteins involved in synaptic transmission and general secretion. J. Neurochem. 66, 889–897.

Hendzel, M.J., Wei, Y., Mancini, M.A., Van Hooser, A., Ranalli, T., Brinkley, B.R., Bazett-Jones, D.P., Allis, C.D., 1997. Mitosis-specific phosphorylation of histone H3 initiates primarily within pericentromeric heterochromatin during G2 and spreads in an ordered fashion coincident with mitotic chromosome condensation. Chromosoma 106, 348–360.

Johnson, S.L., Africa, D., Horne, S., Postlethwait, J.H., 1995. Half-tetrad analysis in zebrafish: mapping the ros mutation and the centromere of linkage group I. Genetics 139, 1727–1735.

Johnson, S.L., Bennett, P., 1999. Growth control in the ontogenetic and regenerating zebrafish fin. Methods Cell Biol. 59, 301–311.

Johnson, S.L., Gates, M.A., Johnson, M., Talbot, W.S., Horne, S., Baik, K., Rude, S., Wong, J.R., Postlethwait, J.H., 1996. Centromere-linkage analysis and consolidation of the zebrafish genetic map. Genetics 142, 1277–1288.

Johnson, S.L., Weston, J.A., 1995. Temperature-sensitive mutations that cause stage-specific defects in Zebrafish fin regeneration. Genetics 141, 1583–1595.

Knapik, E.W., Goodman, A., Atkinson, O.S., Roberts, C.T., Shiozawa, M., Sim, C.U., Weksler-Zangen, S., Trolliet, M.R., Futrell, C., Innes, B.A., Koike, G., McLaughlin, M.G., Pierre, L., Simon, J.S., Vilallonga, E., Roy, M., Chiang, P.W., Fishman, M.C., Driever, W., Jacob, H.J., 1996. A reference cross DNA panel for zebrafish (Danio rerio) anchored with simple sequence length polymorphisms. Development 123, 451–460.

Laforest, L., Brown, C.W., Poleo, G., Geraudie, J., Tada, M., Ekker, M., Akimenko, M.A., 1998. Involvement of the sonic hedgehog, patched 1 and bmp2 genes in patterning of the zebrafish dermal fin rays. Development 125, 4175–4184.

Matsuo, N., Ogawa, S., Takagi, T., Wanaka, A., Mori, T., Matsuyama, T., Pinsky, D.J., Stern, D.M., Tohyama, M., 1997. Cloning of a putative vesicle transport-related protein, RA410, from cultured rat astrocytes and its expression in ischemic rat brain. J. Biol. Chem. 272, 16438–16444.

Mizuta, K., Warner, J.R., 1994. Continued functioning of the secretory pathway is essential for ribosome synthesis. Mol. Cell. Biol. 14, 2493–2502.

Mohammadi, M., McMahon, G., Sun, L., Tang, C., Hirth, P., Yeh, B.K., Hubbard, S.R., Schlessinger, J., 1997. Structures of the tyrosine kinase domain of fibroblast growth factor receptor in complex with inhibitors. Science 276, 955–960.

Montes, G.S., Becerra, J., Toledo, O.M., Gordilho, M.A., Junqueira, L.C., 1982. Fine structure and histochemistry of the tail fin ray in teleosts. Histochemistry 75, 363–376.

Nakagawa, T., Yuan, J., 2000. Cross-talk between two cysteine protease families. Activation of caspase-12 by calpain in apoptosis. J. Cell Biol. 150, 887–894.

Nakagawa, T., Zhu, H., Morishima, N., Li, E., Xu, J., Yankner, B.A., Yuan, J., 2000. Caspase-12 mediates endoplasmic-reticulum-specific apoptosis and cytotoxicity by amyloid-beta. Nature 403, 98–103.

Nechiporuk, A., Finney, J.E., Keating, M.T., Johnson, S.L., 1999. Assessment of polymorphism in zebrafish mapping strains. Genome Res. 9, 1231–1238.

Nechiporuk, A., Keating, M.T., 2002. A proliferation gradient between proximal and msxb-expressing distal blastema directs zebrafish fin regeneration. Development 129, 2607–2617.

Poss, K., Keating, M.T., Nechiporuk, A., 2003. Tales of fin regeneration in zebrafish. Dev. Dyn. 226, 202–210.

Poss, K., Nechiporuk, A., Hillam, A., Johnson, S.L., Keating, M.T., 2002. Mps1 defines a proximal blastemal proliferative compartment essential for zebrafish fin regeneration. Development 129, 5141–5149.

Poss, K.D., Shen, J., Keating, M.T., 2000a. Induction of lef1 during zebrafish fin regeneration. Dev. Dyn. 219, 282–286.

Poss, K.D., Shen, J., Nechiporuk, A., McMahon, G., Thisse, B., Thisse, C., Keating, M.T., 2000b. Roles for Fgf signaling during zebrafish fin regeneration. Dev. Biol. 222, 347–358.

Quint, E., Smith, A., Avaron, F., Laforest, L., Miles, J., Gaffield, W., Akimenko, M.A., 2002. Bone patterning is altered in the regenerating zebrafish caudal fin after ectopic expression of sonic hedgehog and bmp2b or exposure to cyclopamine. Proc. Natl. Acad. Sci. USA 99, 8713–8718.

Ramalho-Santos, M., Yoon, S., Matsuzaki, Y., Mulligan, R.C., Melton, D.A., 2002. "Stemness": transcriptional profiling of embryonic and adult stem cells. Science 298, 597–600.

Shimoda, N., Knapik, E.W., Ziniti, J., Sim, C., Yamada, E., Kaplan, S., Jackson, D., de Sauvage, F., Jacob, H., Fishman, M.C., 1999. Zebrafish genetic map with 2000 microsatellite markers. Genomics 58, 219–232.

Solnica-Krezel, L., Schier, A.F., Driever, W., 1994. Efficient recovery of ENU-induced mutations from the zebrafish germline. Genetics 136, 1401–1420.

Streisinger, G., Walker, C., Dower, N., Knauber, D., Singer, F., 1981. Production of clones of homozygous diploid zebra fish (Brachydanio rerio). Nature 291, 293–296.

Trevarrow, B., Marks, D.L., Kimmel, C.B., 1990. Organization of hindbrain segments in the zebrafish embryo. Neuron 4, 669–679.

Tsonis, P.A., 1996. Limb Regeneration. Cambridge University Press, Cambridge.

Turner, D.L., Weintraub, H., 1994. Expression of achaete-scute homolog 3 in Xenopus embryos converts ectodermal cells to a neural fate. Genes Dev. 8, 1434–1447.

van Eeden, F.J., Granato, M., Odenthal, J., Haffter, P., 1999. Developmental mutant screens in the zebrafish. Methods Cell Biol. 60, 21–41.

Wei, Y., Yu, L., Bowen, J., Gorovsky, M.A., Allis, C.D., 1999. Phosphorylation of histone H3 is required for proper chromosome condensation and segregation. Cell 97, 99–109.

Westerfield, M., 2000. The Zebrafish Book. A Guide for the Laboratory Use of Zebrafish (*Danio rerio*), 4th edition. University of Oregon Press, Eugene, OR.

Yamaguchi, T., Dulubova, I., Min, S.W., Chen, X., Rizo, J., Sudhof, T.C., 2002. Sly1 binds to Golgi and ER syntaxins via a conserved N-terminal peptide motif. Dev. Cell 2, 295–305.

Yoneda, T., Imaizumi, K., Oono, K., Yui, D., Gomi, F., Katayama, T., Tohyama, M., 2001. Activation of caspase-12, an endoplastic reticulum (ER) resident caspase, through tumor necrosis factor receptor-associated factor 2-dependent mechanism in response to the ER stress. J. Biol. Chem. 276, 13935–13940.

Zinszner, H., Kuroda, M., Wang, X., Batchvarova, N., Lightfoot, R.T., Remotti, H., Stevens, J.L., Ron, D., 1998. CHOP is implicated in programmed cell death in response to impaired function of the endoplasmic reticulum. Genes Dev. 12, 982–995.